

Effect of nano-SiO₂ particles on fracture properties of concrete composite containing fly ash

Peng Zhang^{1,*}, Xiao-Bing Dai², Ji-Xiang Gao² and Peng Wang²

¹Open Laboratory of Water Conservancy and Science of Key Disciplines in Henan Province, and

²School of Water Conservancy and Environment Engineering, Zhengzhou University, Zhengzhou 450001, China

A parametric experimental study has been conducted to investigate the effect of nano-SiO₂ particles on fracture properties of concrete composite containing fly ash. Five different nano-SiO₂ contents were used for this study. By means of three-point bending method, the fracture parameters of the effective crack length, initial fracture toughness, unstable fracture toughness, fracture energy, critical crack opening displacement, maximum crack opening displacement and maximum mid-span deflection of the beam specimen were measured. The results reveal that the addition of lower SiO₂ content (<5%) nano-particles may help improve the fracture properties of concrete composite containing fly ash. Nano-SiO₂ has a significant effect on the fracture relational curves of the three-point bending beam specimen. The fracture parameters increase gradually and the fracture relational curves become thicker as the nano-SiO₂ content increases from 0% to 5%. However, the fracture parameters begin to decrease and the curves become thinner when the nano-SiO₂ content exceeds 5%. These variation rules of fracture parameters and fracture relational curves indicate that nano-SiO₂ contributes significantly to the improvement of fracture properties of concrete composite containing fly ash only when its content does not exceed 5%.

Keywords: Three-point bending method, fracture properties, fly ash concrete, nano-SiO₂.

NANOTECHNOLOGY can be considered as the latest field of science and technology. Because nanotechnology has great market potential and economic impact, the need for research and exploration in this field and of its applications has been growing significantly during the last few decades¹. Nanotechnology is also engineering at the nano-scale to produce materials with unique properties that cannot be achieved using traditional materials². Nanomaterials have been considered as the most promising materials in the 21st century by scientists. Nanoparticles have been gaining increasing attention and are being applied in many fields to fabricate new materials with

novel functions due to their unique physical and chemical properties. The extremely high specific surface area is one of the most important characteristics of nanoparticles because it facilitates more interphase in a composite and thereby, a strong interaction between the fillers and the matrix even at a rather low nano-filler loading³. For heterogeneous composites such as concrete composites, addition of nanoparticles makes them an ideal candidate for the application of nanotechnology. Due to the nano-effects of nano-particles such as surface effect, quantum size effect, small size effect and macroscopic quantum tunnelling effect, there is a global interest in the investigation of the influence of nanoparticles on concrete composites. Although the high cost of nanoparticles may prevent their widespread use, they are more advantageous than other admixtures. In recent years, with the reduction of manufacturing cost of nano-materials, many researchers have carried out work on the properties of concrete composites containing nanoparticles.

Woo *et al.*⁴ studied the barrier characteristics of nano-clay composites that were applied onto concrete as a protective coating. The water permeability resistant behaviour and microstructure of concrete with nano-SiO₂ was also experimentally studied^{5,6}. Researchers⁷⁻¹⁰ have also studied the improvement in compressive and flexural strength, abrasion resistance, chloride permeability and flexural fatigue performance of concrete containing nanoparticles. Bahadori and Hosseini¹¹ studied the effects of replacing cement with colloidal amorphous silica nanoparticles on the physical and mechanical properties, durability and microstructure of concrete. Givi *et al.*^{12,13} studied the effects of SiO₂ nanoparticles on both mechanical and physical properties of concrete, and the size effects of SiO₂ nanoparticles on compressive, flexural and tensile strength of binary blended concrete. Nazari and Riahi¹⁴ studied the percentage, rate and coefficient of water absorption, workability and setting time of binary blended concrete with partial replacement of cement by TiO₂ nanoparticles. The results indicate that the addition of nanoparticles to concrete composites improves their mechanical properties and durability.

Nanoparticles can also help improve the properties of concrete composites containing other pozzolanic materials

*For correspondence. (e-mail: zhangpeng8008@gmail.com)

and fibres. The effects of nano-SiO₂ on pore size distribution, rate of hydration, setting time and strength development of concrete with high-volume fly ash and slag have also been studied¹⁵⁻¹⁷. Heidari and Tavakoli¹⁸ studied the compressive strength and water absorption of concrete composite using nano-SiO₂ and waste ground ceramic simultaneously. Najjigivi *et al.*¹⁹ studied the effects of SiO₂ nanoparticles as additives with two different sizes (15 and 80 nm) on water absorption of rice husk ash (RHA) blended concrete. The effects of nano-silica and different fibres on the mechanical and rheological properties and durability of self-compacting concrete were studied and the compressive strength of self-compacting concrete with fibres consisting of nano-SiO₂ was estimated using ultrasonic pulse velocity²⁰⁻²². The results show that there are good prospects of concrete composite containing nanoparticles and other pozzolanic materials and fibres simultaneously.

Fracture properties are extremely important for the safety and durability of structures constructed with concrete composite. The improved pore structure of concrete composite by applying nano-SiO₂ particles causes densification of paste-aggregate transition zone, which in turn affects the fracture properties. Hence, it is necessary to study the effect of nano-SiO₂ particles on fracture properties of concrete composite containing fly ash. However, little information is available regarding this. Zhang *et al.*^{23,24} studied the notch sensitivity of fracture properties of concrete containing nano-SiO₂ particles and fly ash, and the effect of steel fibre on fracture properties of high performance concrete containing nano-SiO₂ particles and fly ash. The results indicate that the relative notch depth of the notched specimens has a significant effect on fracture parameters and the fracture relational curves of concrete containing nano-SiO₂ and fly ash. Also, the addition of appropriate steel fibre content helps improve the fracture properties of high performance concrete containing nano-SiO₂ and fly ash. Therefore, we conducted the present experimental study and measured the fracture toughness, fracture energy, mid-span deflection (δ), crack mouth opening displacement (CMOD) and crack tip opening displacement (CTOD) of the notched beam specimens of concrete composite containing nano-SiO₂ particles to analyse the effect of nano-SiO₂ particles on fracture properties of concrete composite containing fly ash.

Materials and experimental procedure

Raw materials

The cement used was Ordinary Portland cement (Class 42.5R; manufactured by Tianrui Cement Co.) for which the chemical and physical properties are presented in Table 1. Grade I fly ash was used to make the concrete

for which the chemical properties are also presented in Table 1. In this experimental study, amorphous nano-SiO₂ (manufactured by Wanjing New Material Co, Ltd, Hangzhou city, China) with solid content of more than 99% was used. Physical properties of the nanoparticles are presented in Table 2. Nano-SiO₂ content in different series was 1, 3, 5, 7 and 9 wt%. The quantities of fly ash and nano-SiO₂ are expressed as percentages of mass of the cement content. Coarse aggregate with a maximum size of 20 mm and fine aggregate with a 2.76 fineness modulus were used. The specific gravity and silt content of the coarse and fine aggregates were 2.74% and 0.6%, as well as 2.63% and 0.8% respectively. The values of specific gravity of the aggregates in this study are based on saturated surface dry condition. A high-range water reducing agent with commercial name polycarboxylate HJSX-A was used to adjust the workability of the concrete mixture. The performance indices of the high-range water reducing agent are presented in Table 3. The agent was made of many polymer organic compounds, most of which belong to poly carboxylic acid salt. It has great reducing properties with only a small dosage. Besides, the use of this kind of reducing agent in concrete can reduce the slump loss of the concrete. Mix proportions of the concrete composite are given in Table 4. The water-binder ratio (0.32) of each mix proportion remained unchanged in this study.

Preparation of specimens

A series of notched beam specimens with size 100 × 100 × 515 mm were prepared to determine the fracture properties. The beam specimen was sawed from the span centre of the lower surface to produce a pre-cutting crack, with depth of 40 mm. The shape and size of the beam specimen are provided in Figure 1. A photograph of the beam specimen with pre-cutting crack is shown in Figure 2. In order to distribute nano-SiO₂ uniformly, a forced mixing machine was used. The mixing procedure, which

Table 1. Properties of cement and fly ash

Composition (%)	Cement	Fly ash
Chemical composition		
SiO ₂	20.85	51.50
Al ₂ O ₃	5.32	18.46
Fe ₂ O ₃	2.69	6.71
CaO	62.97	8.58
MgO	3.66	3.93
Na ₂ O	0.15	2.52
K ₂ O	0.62	1.85
SO ₃	2.48	0.21
Physical properties		
Specific gravity	3.11	2.16
Specific surface (cm ² /g)	3287	2470

Table 2. Physical properties of nano-SiO₂

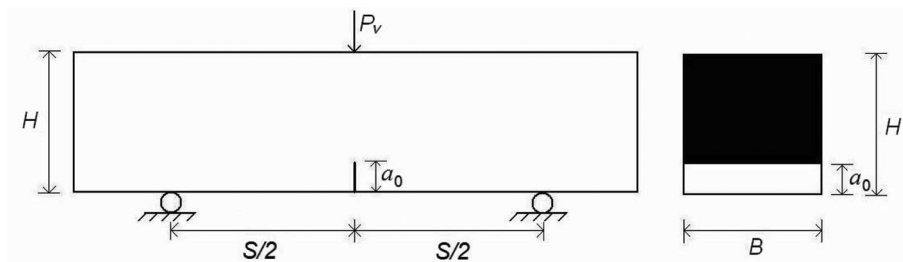
Average particle size (nm)	SiO ₂ content (%)	Specific surface area (m ² /g)	Apparent density (g/cm ³)	pH value
30	99.5	200 ± 10	0.055	5–7

Table 3. Properties of high-range water reducing agent

Solid content (%)	Total alkali content (%)	Fluidity of cement paste (mm)	Density (g/cm ³)	Content of Cl ⁻ (%)	pH value
30	1.2	260	1.052	0.078	4.32

Table 4. Mix proportions of concrete composite

Mix no.	Cement (kg/m ³)	Fly ash (%)	Nano-SiO ₂ (%)	Fine aggregate (kg/m ³)	Coarse aggregate (kg/m ³)	Water (kg/m ³)	Water reducing agent (kg/m ³)
1	419.9	15	0	647	1151	158	4.94
2	414.96	15	1	647	1151	158	4.94
3	405.08	15	3	647	1151	158	4.94
4	395.2	15	5	647	1151	158	4.94
5	385.32	15	7	647	1151	158	4.94
6	375.44	15	9	647	1151	158	4.94

**Figure 1.** Sketch of three-point bending beam specimen.**Figure 2.** Photograph of the beam specimen with pre-cutting crack.

was designed by trial and error, was chosen as follows: the coarse and fine aggregates were mixed initially for 1 min, and cement, fly ash and nano-SiO₂ were mixed for another 2 min. Finally, the high-range water reducing agent and water were added and mixed for 3 min. The

distribution of nano-SiO₂ has a significant effect on the working performance of the mixture and the fracture properties of concrete composite. If nano-SiO₂ is not distributed well, it will be assembled altogether. From the working performance of the mixture and the fracture section of the specimen of the concrete composite, it can be seen that nano-SiO₂ was well distributed in the present study. After casting, all the upper surfaces of the specimens were smoothed using a steel towel. Immediately after smoothed, the specimens were covered with plastic sheets to minimize moisture loss. All the specimens were stored at about 23°C in a casting room. They were demoulded after 24 h, and then cured at 100% relative humidity and controlled temperature (21° ± 2°C) for 28 days before testing.

Experimental method

In this study, three-point bending beam method was employed to measure the fracture parameters, which is an appropriate fracture testing method recommended by the Committee on Fracture Mechanics of Concrete of the International Union of Laboratories and Experts in

Construction Materials, Systems and Structures²⁵. The experiment was carried out on a hydraulic pressure testing machine, whose measure range of the load transducer is 0–30 kN. CMOD and CTOD were measured by clamp-type extended instruments. CMOD can be defined as the increase in the crack width of the pre-cutting crack mouth during the course of loading and CTOD can be defined as the increase in the crack length of the pre-cutting crack during the course of loading. The mid-span deflection (δ) of the beam specimen was measured using a displacement meter fixed on one side of the specimen by an angle bracket. During the course of testing, the loading was kept continual and consistent, and the loading rate was reduced slightly when the specimen was approaching failure. The relational curves between the vertical load and the mid-span deflection ($P_V - \delta$) crack mouth opening displacement ($P_V - \text{CMOD}$) and crack tip opening displacement ($P_V - \text{CTOD}$) were obtained respectively, from the $X - Y$ dynamic function recorder. The testing apparatus of fracture test is presented in Figure 3.

Determination of fracture parameters

In this study, the fracture properties of concrete composite containing nano-SiO₂ were evaluated by the double- K fracture parameters (initial fracture toughness K_{IC}^{ini} and unstable fracture toughness K_{IC}^{un})²⁶, and fracture energy G_F . The propagation length of the crack is needed for the calculation of K_{IC}^{ini} and K_{IC}^{un} . The higher K_{IC}^{ini} and K_{IC}^{un} values indicate that the concrete is more resistant to crack expansion and has better fracture properties. On the contrary, the concrete composite exhibits poor fracture properties with lower values of K_{IC}^{ini} and K_{IC}^{un} . The actual length of the crack is more than the depth of the pre-cutting crack of the specimen because there is a stage of steady expansion before unstable fracture occurs, and the propagation length of the crack is the difference between



Figure 3. Loading device of three-point bending test.

the actual length of the crack and depth of the pre-cutting crack of the specimen. However, it is difficult to accurately measure the actual length of the crack. Therefore, the effective crack length of the three-point bending beam specimen is generally used to calculate K_{IC}^{ini} and K_{IC}^{un} . The effective crack length can be calculated as follows²⁷

$$a_c = \frac{2}{\pi} H \times \arctan \sqrt{\frac{EB}{32.6P_{V_{max}}} \text{CMOD}_c - 0.1135}, \quad (1)$$

where a_c is the effective crack length of the three-point bending beam specimen (m), $P_{V_{max}}$ the peak vertical load (kN), CMOD_c the critical crack mouth opening displacement (m), E the elastic modulus of the concrete composite (MPa), H the height of the beam specimen (m) and B is the width of the beam specimen (m).

With the measured initial cracking load and the depth of the pre-cutting crack of the three-point bending beam specimen, the initial fracture toughness of concrete composite containing nano-SiO₂ can be calculated as follows²⁸

$$K_{IC}^{ini} = \frac{3P_{ini}S\sqrt{a_0}}{2BH^2} f\left(\frac{a_0}{H}\right), \quad (2)$$

where K_{IC}^{ini} is the initial fracture toughness (kN/m^{3/2}), P_{ini} the initial cracking load (kN), S the span length of the beam specimen (m), H the height of the beam specimen (m), B the width of the beam specimen (m) and a_0 is the depth of the pre-cutting crack of the three-point bending beam specimen (m). $f(a_0/H)$ is a function relevant to a_0/H , which can be expressed as follows

$$f\left(\frac{a_0}{H}\right) = \frac{1.99 - \frac{a_0}{H} \left(1 - \frac{a_0}{H}\right) \left[2.15 - 3.93 \frac{a_0}{H} + 2.7 \left(\frac{a_0}{H}\right)^2 \right]}{\left(1 + 2 \frac{a_0}{H}\right) \left(1 - \frac{a_0}{H}\right)^{1.5}}. \quad (3)$$

With the measured peak vertical load and the effective crack length of the three-point bending beam specimen, the unstable fracture toughness of concrete composite containing nano-SiO₂ can be calculated as follows²⁸

$$K_{IC}^{un} = \frac{3P_{V_{max}}S\sqrt{a_c}}{2BH^2} f\left(\frac{a_c}{H}\right), \quad (4)$$

where K_{IC}^{un} is the unstable fracture toughness (kN/m^{3/2}), $P_{V_{max}}$ the peak vertical load (kN), S the span length of the beam specimen (m), H the height of the beam specimen (m), B the width of the beam specimen (m), a_c is the effective crack length of the three-point bending beam

specimen (m). $f(a_c/H)$ is a function relevant to a_c/H which can be expressed as follows

$$f\left(\frac{a_c}{H}\right) = \frac{1.99 - \frac{a_c}{H} \left(1 - \frac{a_c}{H}\right) \left[2.15 - 3.93 \frac{a_c}{H} + 2.7 \left(\frac{a_c}{H}\right)^2\right]}{\left(1 + 2 \frac{a_c}{H}\right) \left(1 - \frac{a_c}{H}\right)^{1.5}} \quad (5)$$

The fracture energy results from integration of the load-displacement curve per unit of the fractured surface of the specimen²⁹. With the measured ultimate mid-span deflection and the relational curve of $P_V - \delta$ of the three-point bending beam specimen, the fracture energy of concrete composite containing nano-SiO₂ can be calculated as follows³⁰

$$G_F = \frac{1}{A_{\text{lig}}} [W_0 + (m_1 + 2m_2)g\delta_{\text{max}}], \quad (6)$$

$$A_{\text{lig}} = B(H - a_0), \quad (7)$$

where G_F is the fracture energy (N/m), A_{lig} the area of the fracture ligament of the specimen (m²), H the height of the beam specimen (m), B the width of the beam specimen (m), a_0 the depth of the notched crack (m), g the gravitational acceleration ($g = 9.8 \text{ m/s}^2$); m_1 the weight of the specimen between the two supports (kg); m_2 the additive weight of the loading facilities (kg); δ_{max} the maximum mid-span deflection of the beam specimen (m) and W_0 is the area above the axis of δ and under the relational curve of $P_V - \delta$ (Nm; Figure 4). There are six specimens for each proportion, and the average of the six values of calculation is taken as the final result.

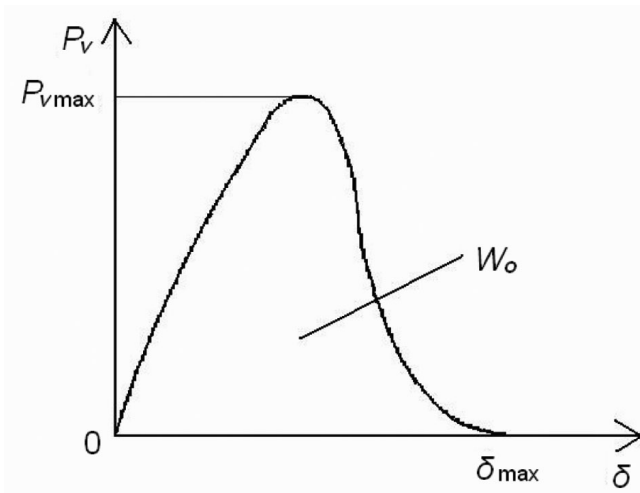


Figure 4. Full curve of $P_V - \delta$.

Results and discussion

Effect of nano-SiO₂ on fracture toughness

The results of the effective crack length (a_c) of the three-point bending beam specimens of nano-SiO₂ reinforced concrete composite containing 15% fly ash, with the curing period of 28 days, are shown in Figure 5. The results show that a_c increases with SiO₂ nanoparticles up to 5% replacement of the cement and then it decreases, although 9% replacement of the cement is still higher than that of the concrete composite only containing 15% fly ash. Compared with the concrete composites without nano-SiO₂, the increase of a_c is determined as 7.2% for the concrete composite with 5% nano-SiO₂.

Figure 6a and b shows the variation rules of initial fracture toughness ($K_{\text{IC}}^{\text{ini}}$) and unstable fracture toughness ($K_{\text{IC}}^{\text{un}}$) of concrete composite with 15% fly ash at 28 days curing period with increase in nano-SiO₂ content respectively. As expected, in general, the concrete composite specimens made with SiO₂ nanoparticles show higher $K_{\text{IC}}^{\text{ini}}$ and $K_{\text{IC}}^{\text{un}}$ than those made without SiO₂ nanoparticles. Both $K_{\text{IC}}^{\text{ini}}$ and $K_{\text{IC}}^{\text{un}}$ increase gradually with the increase in nano-SiO₂ content, when it is below 5%. However, just like a_c of the three-point bending beam specimens, $K_{\text{IC}}^{\text{ini}}$ and $K_{\text{IC}}^{\text{un}}$ begin to decrease with the continued increase of nano-SiO₂ content when it exceeds 5%. The variations of a_c , $K_{\text{IC}}^{\text{ini}}$ and $K_{\text{IC}}^{\text{un}}$ indicate that lower content of SiO₂ nanoparticles helps improve the fracture properties of the concrete composite containing fly ash compared to higher SiO₂ nanoparticles content. This may be due to the fact that the quantity of SiO₂ nanoparticles present in the mix is higher than the amount required to combine with the liberated lime during the process of hydration, thus leading to excess silica leaching out and causing a deficiency in strength as it replaces part of the

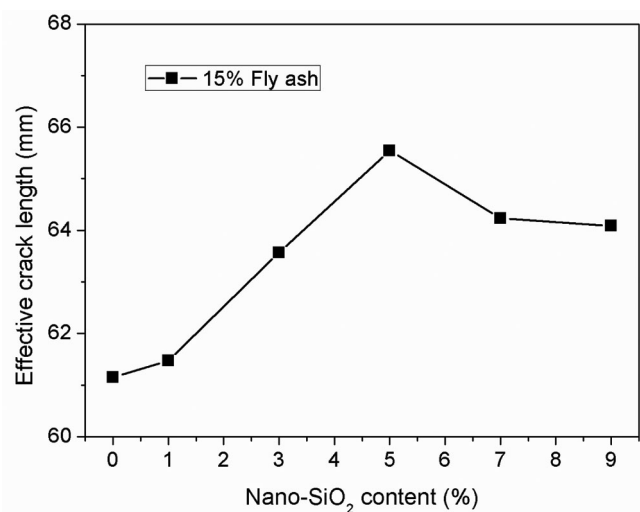


Figure 5. Effect of nano-SiO₂ content on effective crack length.

cementitious material but does not contribute to its strength³¹.

Effect of nano-SiO₂ on fracture energy

The variations of G_F of nano-SiO₂ reinforced concrete composite containing 15% fly ash with 1%, 3%, 5%, 7% and 9% cement replacement with nano-SiO₂ at 28 days curing period are illustrated in Figure 7. From the results, it can be seen that all the concrete composites containing nano-SiO₂ have higher G_F than the concrete composite without nanoparticles. A considerable increase in G_F of the concrete composite was observed by increasing the nano-SiO₂ content, when it is not beyond 5%. Compared with the control mix without nanoparticles, the increase in G_F was determined as 24.3%, 38.1% and 67.3% for 1%, 3% and 5% cement replacement with nano-SiO₂ respectively. However, as the nano-SiO₂ content increases continuously, further decrease in G_F is observed. The fracture energy G_F of concrete composite is a basic material characteristic, representing the energy necessary

to create a unit area of fracture surface. The higher G_F indicates that more energy will be consumed to make the concrete composite fracture and the concrete composite has better fracture properties. On the contrary, the concrete composite shows poor fracture properties with lower G_F .

Figure 8 presents the typical complete curves of $P_V - \delta$ of the three-point bending beam specimens of concrete composite containing 15% fly ash with different nano-SiO₂ contents, as well as a curve obtained for the concrete composite containing 15% fly ash without nano-SiO₂. From the figure, it can be seen that the relational curve of $P_V - \delta$ becomes thicker, the nonlinear stage of the curve becomes longer and the descent stage of the curve is more gradual when the nano-SiO₂ content increases from 0% to 5%, while the relational curve becomes thinner, when the nano-SiO₂ content increases from 5% to 9%. Figure 9 shows the variation of the maximum mid-span deflection (δ_{max}) of the three-point bending beam specimens with increase in nano-SiO₂ content. As can be seen from the figure, in general, the maximum mid-span deflection becomes larger when the

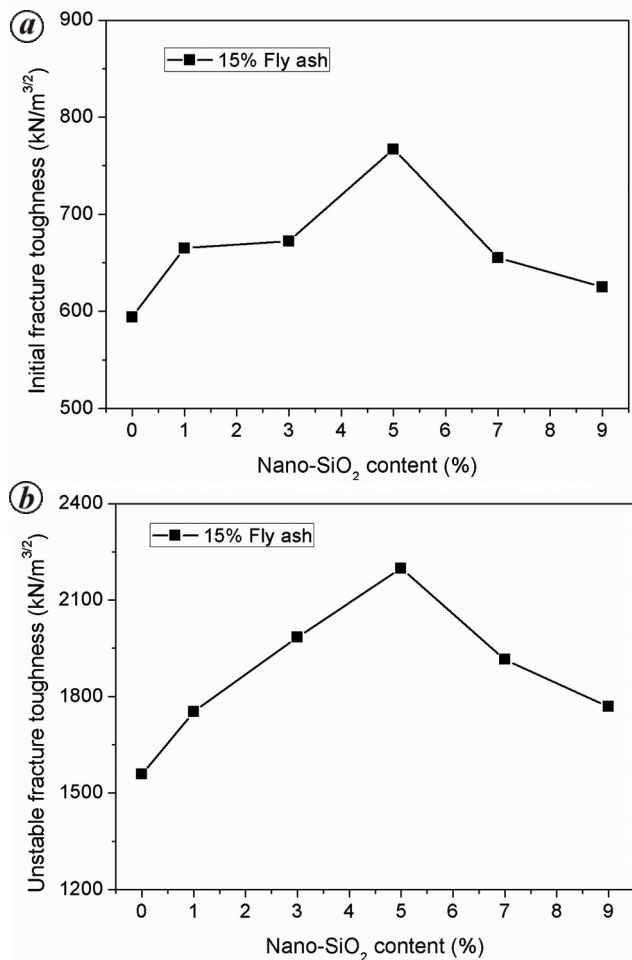


Figure 6. Effect of nano-SiO₂ content on (a) initial fracture toughness and (b) unstable fracture toughness.

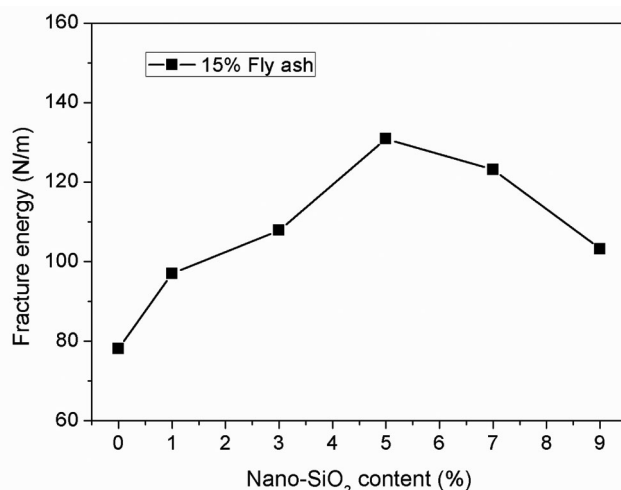


Figure 7. Effect of nano-SiO₂ content on fracture energy.

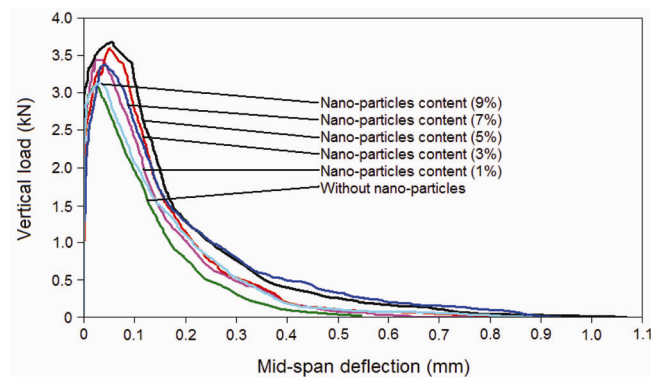


Figure 8. $P_V - \delta$ curves for different nano-SiO₂ contents.

nano-SiO₂ content increases from 0% to 5%, while it becomes smaller when the nano-SiO₂ content increases from 5% to 9%. For concrete composite, the thicker and longer relational curve of $P_V - \delta$ indicates that the three-point bending beam specimen has better fracture properties³⁰. Accordingly, the variation rules of the relational curves of $P_V - \delta$ and the maximum mid-span deflection indicate that the resistance to crack propagation of concrete composite containing fly ash gradually increases with the increase in nano-SiO₂ content as the fracture

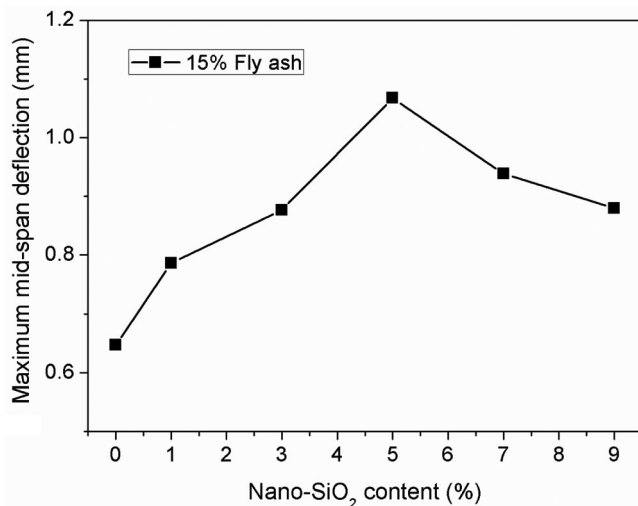


Figure 9. Effect of nano-SiO₂ content on maximum mid-span deflection.

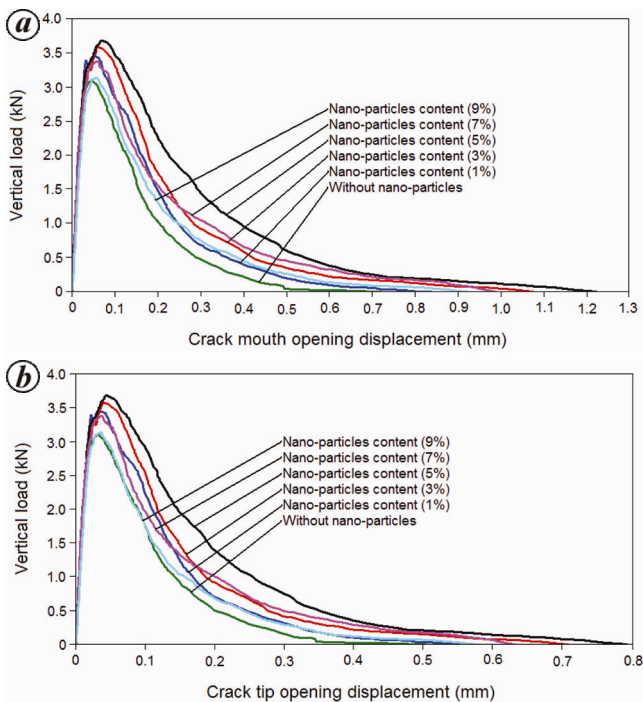


Figure 10. $P_V - \text{CMOD}$ (a) and $P_V - \text{CTOD}$ (b) curves for different nano-SiO₂ contents.

properties are seen to improve with nano-SiO₂ content not beyond 5%.

Few studies have been conducted on fracture properties of cementitious composite reinforced by SiO₂ nanoparticles and some possible reasons have been represented to show the increment of G_F . When a small amount of the nanoparticles is uniformly dispersed in the cement paste, the nanoparticles act as a nucleus to tightly bind with cement hydrate and further promote cement hydration due to their high activity, which is favourable for the strength of cement mortar^{32,33}. Besides, the nanoparticles among the hydrate products will prevent crystals from growing which are not favourable for the strength of cement paste^{33,34}. The nanoparticles fill the cement pores, thus increasing its strength. Nano-SiO₂ can contribute to the hydration process to generate more C-S-H through reaction with Ca(OH)₂ (ref. 12).

Effect of nano-SiO₂ on CMOD and CTOD

The different relational curves of $P_V - \text{CMOD}$ and $P_V - \text{CTOD}$ of the three-point bending beam specimens of the concrete composites reinforced with SiO₂ nanoparticles at 28 days curing period with the increase of nano-SiO₂ content are given in Figure 10 a and b respectively. From the figure, it can be seen that the effect of nano-SiO₂ content on the curves is significant; and both types of curves become thicker with the increase in nano-SiO₂ content, when it increases from 0% to 5%, while the curves become thinner when nano-SiO₂ content exceeds 5%. Figure 11 a and b shows the variations of the critical crack opening displacement (CMOD_c and CTOD_c) and the maximum crack opening displacement (CMOD_{max} and CTOD_{max}) of concrete composites containing fly ash for different nano-SiO₂ contents respectively. CMOD_c can be defined as the crack mouth opening displacement when the vertical load reaches the maximum value³⁵. Similarly, CTOD_c can be defined as the crack tip opening displacement when the vertical load reaches the maximum value. CMOD_{max} can be defined as the maximum crack mouth opening displacement when the specimen is destroyed. Similarly, CTOD_{max} can be defined as the maximum crack tip opening displacement when the specimen is destroyed. It can be generally seen that the effect of SiO₂ nanoparticles on the crack opening displacement is significant, CMOD and CTOD increase gradually as the nano-SiO₂ content increases from 0% to 5%, while they begin to decrease when the nano-SiO₂ content exceeds 5%. Compared with the concrete composite containing no SiO₂ nanoparticles, the increase of CMOD_c and CTOD_c was determined as 45% and 44.3% respectively, and the increase of CMOD_{max} and CTOD_{max} was estimated as 69.9% and 60.7% respectively, for concrete composite with 5% replacement of cement. From the results of CMOD and CTOD, it can also be seen that the contribution of

SiO₂ nanoparticles to the fracture properties of concrete composite containing fly ash is significant only when the nano-SiO₂ content does not exceed 5%.

The reason why the addition of nano-SiO₂ improves the fracture properties of concrete composites containing fly ash may be closely related to the specific nanometre effect of the nano-SiO₂ particles. These particles possess high specific surface area and can react with Ca(OH)₂ to produce C-S-H condensed gel. Hence, during a pozzolanic reaction, the number and size of crystals of Ca(OH)₂ are reduced and C-S-H gel, produced by the pozzolanic reaction, forms a denser transition zone¹¹. The extremely fine particle size of nano-SiO₂ may have accelerated cement and fly ash hydration by providing more nucleation sites for precipitation of cement hydration products in the fly ash concrete composites. In addition to the nucleation effect, nano-SiO₂ may have acted as reactive filler which reduces bleeding and increases packing density of solid materials by occupying space between cement and fly ash particles¹⁷. With the presence of nanoparticles and fly ash, the pozzolanic reaction will be more complete inside

the concrete composites, and the rate of the pozzolanic reaction will be higher. Thus the change of the pozzolanic reaction with the addition of nanoparticles helps improve the fracture properties of the concrete composites. Furthermore, the addition of nano-SiO₂ makes the concrete composite denser and improves its bearing capacity; there is a decrease in the size and number of microcracks inside the concrete composite. The particles of nano-SiO₂ can form a special network structure to prevent the microcracks expanding. Therefore, the fracture properties of concrete composites can be improved.

Conclusions

This article reported experimental results of fracture property studies conducted on nano-SiO₂ reinforced concrete composite containing fly ash. SiO₂ nanoparticles help significantly improve fracture parameters of K_{IC} , G_F , δ_{max} , $CMOD_c$, $CTOD_c$, $CMOD_{max}$ and $CTOD_{max}$ of concrete composite containing fly ash. The results also showed that nano-SiO₂ has an effect on the relational curves of $P_V - \delta$, $P_V - CMOD$ and $P_V - CTOD$ of the three-point bending beam specimen. When the nano-SiO₂ content increased from 0% to 5%, the fracture parameters increased gradually and the fracture relational curves became thicker with the increase in nano-SiO₂ content. However the fracture parameters began to decrease and the curves became thinner when nano-SiO₂ content exceeded 5%. The variation rules of fracture parameters and fracture relational curves indicate that the contribution of nano-SiO₂ to the improvement of fracture properties of concrete composite containing fly ash is significant only when the nano-SiO₂ content does not exceed 5%.

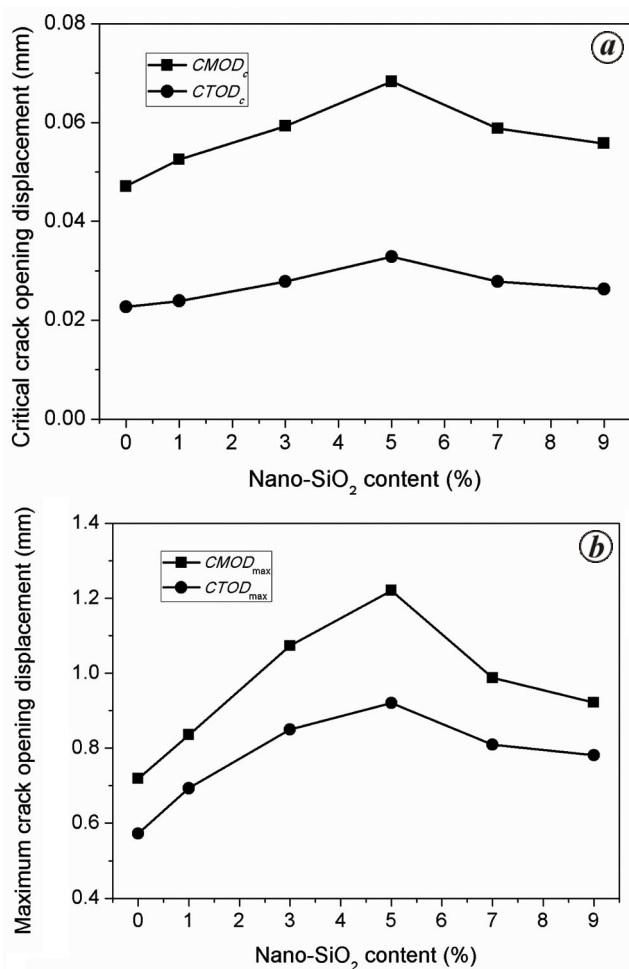


Figure 11. Effect of nano-SiO₂ content on (a) critical crack opening displacement and (b) maximum crack opening displacement.

1. Said, A. M., Zeidan, M. S., Bassuoni, M. T. and Tian, Y., Properties of concrete incorporating nano-silica. *Concr. Build. Mater.*, 2012, **36**, 838–844.
2. Gopinath, S., Mouli, P. C., Murthy, A. R., Iyer, N. R. and Maheswaran, S., Effect of nano silica on mechanical properties and durability of normal strength concrete. *Arch. Civ. Eng.*, 2012, **4**, 433–444.
3. Zhang, G., Chang, L. and Schlarb, A. K., The roles of nano-SiO₂ particles on the tribological behavior of short carbon fiber reinforced PEEK. *Compos. Sci. Technol.*, 2009, **69**, 1029–1035.
4. Woo, R. S. C., Zhu, H., Chow, M. M. K., Leung, C. K. Y. and Kim, J., Barrier performance of silane-clay nanocomposite coatings on concrete structure. *Compos. Sci. Technol.*, 2008, **68**, 2828–2836.
5. Ji, T., Preliminary study on the water permeability and microstructure of concrete incorporating nano-SiO₂. *Cem. Concr. Res.*, 2005, **35**, 1943–1947.
6. Givi, A. N., Rashid, S. A., Aziz, F. N. A. and Salleh, M. A. M., Investigations on the development of the permeability properties of binary blended concrete with nano-SiO₂ particles. *J. Compos. Mater.*, 2011, **45**, 1931–1938.
7. Li, H., Zhang, M. H. and Ou, J. P., Abrasion resistance of concrete containing nano-particles for pavement. *Wear*, 2006, **260**, 1262–1266.

8. Li, H., Zhang, M. H. and Ou, J. P., Flexural fatigue performance of concrete containing nano-particles for pavement. *Int. J. Fatigue*, 2007, **29**, 1291–1301.
9. Shekari, A. H. and Razzaghi, M. S., Influence of nano particles on durability and mechanical properties of high performance concrete. *Procedia Eng.*, 2011, **14**, 3036–3041.
10. Zhang, M. H. and Li, H., Pore structure and chloride permeability of concrete containing nano-particles for pavement. *Constr. Build. Mater.*, 2011, **25**, 608–616.
11. Bahadori, H. and Hosseini, P., Modeling reduction of cement consumption by the aid of silica nano-particles (investigation on concrete properties). *J. Civ. Eng. Manage.*, 2012, **18**, 416–425.
12. Givi, A. N., Rashid, S. A., Aziz, F. N. A. and Salleh, M. A. M., Experimental investigation of the size effects of SiO₂ nano-particles on the mechanical properties of binary blended concrete. *Compos. Part B: Eng.*, 2010, **41**, 673–677.
13. Givi, A. N., Rashid, S. A., Aziz, F. N. A. and Salleh, M. A. M., The effects of lime solution on the properties of SiO₂ nanoparticles binary blended concrete. *Compos. Part B: Eng.*, 2011, **42**, 562–569.
14. Nazari, A. and Riahi, S., The effects of TiO₂ nanoparticles on properties of binary blended concrete. *J. Compos. Mater.*, 2010, **45**, 1181–1188.
15. Zhang, M. H. and Islam, J., Use of nano-silica to reduce setting time and increase early strength of concretes with high volumes of fly ash or slag. *Constr. Build. Mater.*, 2012, **29**, 573–580.
16. Li, G., Use of properties of high-volume fly ash concrete incorporating nano-SiO₂. *Cem. Concr. Res.*, 2004, **34**, 1043–1049.
17. Zhang, M. H., Islam, J. and Peethamparan, S., Use of nano-silica to increase early strength and reduce setting time of concretes with high volumes of slag. *Cem. Concr. Compos.*, 2012, **34**, 650–662.
18. Heidari, A. and Tavakoli, D., A study of the mechanical properties of ground ceramic powder concrete incorporating nano-SiO₂ particles. *Constr. Build. Mater.*, 2013, **38**, 255–264.
19. Najjigivi, A., Rashid, S. A., Aziz, F. N. A. and Salleh, M. A. M., Water absorption control of ternary blended concrete with nano-SiO₂ in presence of rice husk ash. *Mater. Struct.*, 2012, **45**, 1007–1017.
20. Beigi, M. H., Berenjian, J., Omran, O. L., Nik, A. S. and Nikbin, I. M., An experimental survey on combined effects of fibers and nanosilica on the mechanical, rheological, and durability properties of self-compacting concrete. *Mater. Des.*, 2013, **50**, 1019–1029.
21. Nik, A. S. and Omran, O. L., Estimation of compressive strength of self-compacted concrete with fibers consisting nano-SiO₂ using ultrasonic pulse velocity. *Constr. Build. Mater.*, 2013, **44**, 654–662.
22. Khalaj, G. and Nazari, A., Modeling split tensile strength of high strength self compacting concrete incorporating randomly oriented steel fibers and SiO₂ nanoparticles. *Compos. Part B: Eng.*, 2012, **43**, 1887–1892.
23. Zhang, P., Guan, Q. Y., Liu, C. H., Zhang, T. H. and Wang, P., Study on notch sensitivity of fracture properties of concrete containing nano-SiO₂ particles and fly ash. *J. Nanomater.*, 2013, **2013**, 1–7.
24. Zhang, P., Liu, C. H., Li, Q. F., Zhang, T. H. and Wang, P., Fracture properties of steel fibre reinforced high-performance concrete containing nano-SiO₂ and fly ash. *Curr. Sci.*, 2014, **106**, 980–987.
25. RILEM 50-FMC, Determination of fracture energy of mortar and concrete by means of three-point bend tests on notched beams. *Mater. Struct.*, 1985, **18**, 287–290.
26. Xu, S. and Reinhardt, H. W., A simplified method for determining double-K fracture parameters for three-point bending tests. *Int. J. Fract.*, 2000, **104**, 181–209.
27. Xu, S. L., Wu, Z. M. and Ding, S. G., A practical analytical approach to the determination of double-K fracture parameters of concrete. *Eng. Mech.*, 2003, **20**, 54–61.
28. Rong, H., Dong, W., Wu, Z. M. and Fan, X. L., Experimental investigation on double-K fracture parameters for large initial crack-depth ratio in concrete. *Eng. Mech.*, 2012, **29**, 162–167.
29. Elser, M., Tschegg, E. K., Finger, N. and Stanzl-Tschegg, S. E., Fracture behaviour of polypropylene-fiber-reinforced concrete: modeling and computer simulation. *Compos. Sci. Technol.*, 1996, **56**, 947–956.
30. Yu, Y. Z., Zhang, Y. M., Guo, G. L., Rao, B. and Zhou, J. C., Study on fracture energy G_F of concrete. *Shuili Xuebao*, 1987, **18**, 300–307.
31. Al-Khalaf, M. N. and Yousift, H. A., Use of rice husk ash in concrete. *Int. J. Cem. Compos. Lightweight Concr.*, 1984, **6**, 241–248.
32. Li, H., Xiao, H. G., Yuan, J. and Ou, J. P., Microstructure of cement mortar with nanoparticles. *Compos. Part B: Eng.*, 2004, **35**, 185–189.
33. Li, H., Xiao, H. and Ou, J. P., A study on mechanical and pressure-sensitive properties of cement mortar with nanophase materials. *Cem. Concr. Res.*, 2004, **34**, 435–438.
34. Grzeszczyk, S. and Lipowski, G., Effect of content and particle size distribution of high calcium fly ash on the rheological properties of cement pastes. *Cem. Concr. Res.*, 1997, **27**, 907–916.
35. Zhang, P., Liu, C. H., Li, Q. F. and Zhang, T. H., Effect of polypropylene fiber on fracture properties of cement treated crushed rock. *Compos. Part B: Eng.*, 2013, **55**, 48–54.

ACKNOWLEDGEMENTS. We thank the National Natural Science Foundation of China (51208472) and Open Laboratory of Water Conservancy and Science of Key Disciplines in Henan Province, Zhengzhou University for financial support.

Received 21 June 2014; revised accepted 14 March 2015